PNAS RESEARCH ARTICLE | PLANT BIOLOGY

Elucidation of tropane alkaloid biosynthesis in *Erythroxylum coca* using a microbial pathway discovery platform

Benjamin G. Chavez[a,1], Prashanth Srinivasan[b,1], Kayla Glockzin[c], Neill Kim[c], Olga Montero Estrada[c], Jan Jirschitzka[d], Gage Rowden[c], Jonathan Shao[e], Lyndel Meinhardt[e], Christina D. Smolke[b,f,2], and John C. D'Auria[a,2]

Edited by Ian Baldwin, Max-Planck-Institut fur chemische Okologie Abteilung fur Molekulare Okologie, Jena, Germany; received September 14, 2022; accepted October 25, 2022

Tropane alkaloids (TAs) are heterocyclic nitrogenous metabolites found across seven orders of angiosperms, including Malpighiales (Erythroxylaceae) and Solanales (Solanaceae). Despite the well-established euphorigenic properties of Erythroxylaceae TAs like cocaine, their biosynthetic pathway remains incomplete. Using yeast as a screening platform, we identified and characterized the missing steps of TA biosynthesis in *Erythroxylum coca*. We first characterize putative *E. coca* polyamine synthase- and amine oxidase-like enzymes in vitro, in yeast, and in planta to show that the first tropane ring closure in Erythroxylaceae occurs via bifunctional spermidine synthase/*N*-methyltransferases and both flavin- and copper-dependent amine oxidases. We next identify a SABATH family methyltransferase responsible for the 2-carbomethoxy moiety characteristic of Erythroxylaceae TAs and demonstrate that its coexpression with methylecgonone reductase in yeast engineered to express the Solanaceae TA pathway enables the production of a hybrid TA with structural features of both lineages. Finally, we use clustering analysis of *Erythroxylum* transcriptome datasets to discover a cytochrome P450 of the CYP81A family responsible for the second tropane ring closure in Erythroxylaceae, and demonstrate the function of the core coca TA pathway in vivo via reconstruction and de novo biosynthesis of methylecgonine in yeast. Collectively, our results provide strong evidence that TA biosynthesis in Erythroxylaceae and Solanaceae is polyphyletic and that independent recruitment of unique biosynthetic mechanisms and enzyme classes occurred at nearly every step in the evolution of this pathway.

convergent evolution | *N*-methylspermidine | pathway discovery | tropane alkaloid | Erythroxylaceae

Significance

We used a yeast platform to identify all unaccounted enzymatic steps of the tropane alkaloid biosynthetic pathway in Erythroxylaceae. We provide multiple lines of evidence that biosynthesis of tropane alkaloids independently arose at least twice during the evolution of land plants. The coca pathway includes an alternative route for the biosynthesis of critical polyamines, as well as the missing enzymes responsible for the second ring closure and formation of the 2-carbomethoxy moiety, which is exclusive to Erythroxylaceae and responsible in part for the euphorigenic properties of its alkaloids. Our work demonstrates unique enzyme families were independently recruited at nearly every step of the tropane alkaloid pathway, providing insights into the development of biosynthetic diversity in angiosperms.

Tropane alkaloids (TAs) are a diverse class of plant-specialized metabolites (1). These heterocyclic nitrogenous compounds are identified by their *N*-methyl-8-azabicyclo[3.2.1]-octane core structure, found in more than 200 unique alkaloids (1–3). TAs are synthesized in seven plant orders with scattered distribution across angiosperms, including Malpighiales (Erythroxylaceae) and Solanales (Solanaceae) (4, 5). TAs possess varied pharmaceutical properties and are often used as starter molecules for drug development (2). The methylated nitrogen of the TA core is analogous to acetylcholine and can competitively inhibit the muscarinic acetylcholine receptors (6). One of the most infamous TAs is cocaine, exclusively found in the leaves of *Erythroxylum coca* and *Erythroxylum novogranatense* (7–9). TAs of the Erythroxylaceae, including cocaine, are characterized by a 3β stereospecific conformation and binding of the aromatic ring at the 3β position to specific receptor sites blocks reuptake of norepinephrine, serotonin, and dopamine, explaining their anesthetic and euphorigenic properties (10–12). In contrast, two of the most pharmacologically important TAs of the Solanaceae, atropine and scopolamine, possess an aromatic ring with a 3α configuration (13). The World Health Organization considers these TAs as essential medicines as they and their semi-synthetic derivatives are used to treat a range of diseases, including post-operative nausea, tremors, motion sickness, and chronic obstructive pulmonary disease (14).

TA biosynthesis occurs in three stages: 1) the first nitrogen-containing heterocyclic ring closure, 2) the second ring closure forming the bicyclic TA core scaffold, and 3) modifications via the addition of functional groups to the bicyclic core. Although TA biosynthesis has predominantly been studied in Solanaceae, multiple lines of evidence point towards an independent evolution of TA biosynthesis in Erythroxylaceae (2). Examples of this independent evolution are found in the enzyme classes and catalytic mechanisms of characterized steps in TA biosynthesis (Fig. 1). Methylecgonone reductase (*Ec*MecgoR) belongs to the aldo-keto reductase family of enzymes instead of the short-chain dehydrogenases/reductases, which include the tropinone reductases (TRs) found in Solanaceae (1). Erythroxylaceae 3-oxoglutaric acid synthase (*Ec*OGAS, previously referred to as pyrrolidine

Author contributions: B.G.C., P.S., C.D.S., and J.C.D. designed research; B.G.C., P.S., K.G., N.K., O.M.E., J.J., G.R., C.D.S., and J.C.D. performed research; B.G.C., P.S., K.G., N.K., O.M.E., J.J., G.R., J.S., L.M., C.D.S., and J.C.D. analyzed data; and B.G.C., P.S., K.G., N.K., O.M.E., J.J., G.R., J.S., L.M., C.D.S., and J.C.D. wrote the paper.

The authors declare no competing interest.

This article is a PNAS Direct Submission.

[1]B.G.C and P.S. contributed equally to this work.

[2]To whom correspondence may be addressed. Email: csmolke@stanford.edu or dauria@ipk-gatersleben.de.

This article contains supporting information online at https://www.pnas.org/lookup/suppl/doi:10.1073/pnas.2215372119/-/DCSupplemental.

Published November 28, 2022.

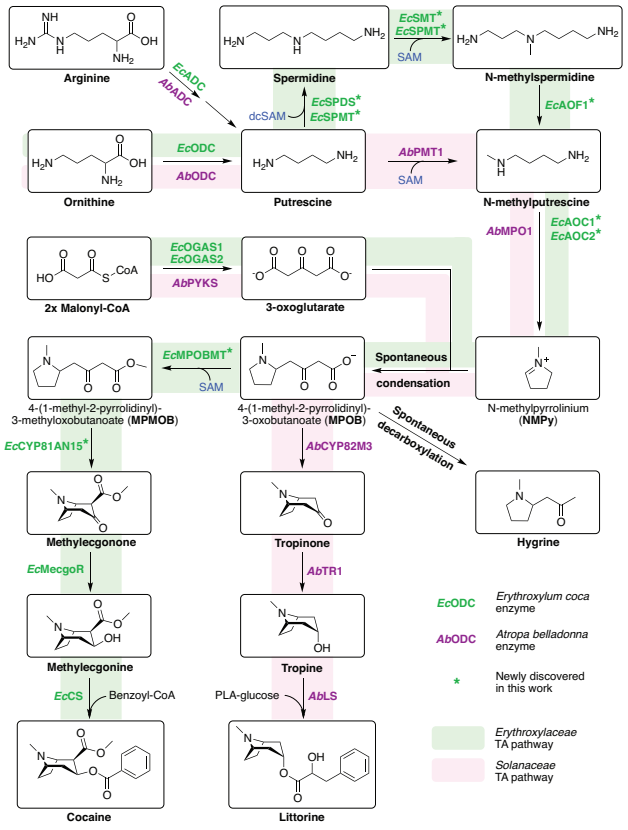

Fig. 1. Independent evolution of TA biosynthetic pathways in Erythroxylaceae and Solanaceae. Erythroxylaceae and Solanaceae gene names and biosynthetic routes are indicated in green and magenta, respectively. Enzyme cofactors and cosubstrates are indicated in blue. Gene abbreviations: ADC, arginine decarboxylase; SMT, spermidine *N*-methyltransferase; SPMT, bifunctional spermidine synthase/*N*-methyltransferase; AOF, flavin-dependent amine oxidase; AOC, copper-dependent amine oxidase; PMT, putrescine *N*-methyltransferase; OGAS, 3-oxoglutarate synthase; PYKS, pyrrolidine ketide synthase; MPOBMT, MPOB methyltransferase; CYP82M3, tropinone synthase; CYP81AN15, methylecgonone synthase; MecgoR, methylecgonone reductase; LS, littorine synthase; CS, cocaine synthase. *Indicates genes newly identified in this study.

ketide synthase or PKS/PYKS based on its Solanaceae analogs) does not directly synthesize 4-(1-methyl-2-pyrrolidinyl)-3-oxobutanic acid (MPOB) from the *N*-methyl-Δ^1-pyrrolinium cation (NMPy) and malonyl-CoA but instead forms 3-oxoglutaric acid from two units of malonyl-CoA (Fig. 1). While similar type III polyketide synthases responsible for this step are found in Solanaceae, recent evidence indicates these enzymes are the products of repeated evolution and have independently evolved within their respective lineages (15, 16). Erythroxylaceae and Solanaceae have also recruited different acyltransferase families for the esterification of the tropane ring. In *E. coca,* the last step of cocaine biosynthesis is catalyzed by a BAHD acyltransferase called cocaine synthase (*Ec*CS), which condenses coenzyme A (CoA) thioesters like benzoyl-CoA with methylecgonine (17, 18). In contrast, Solanaceae such as *Atropa belladonna* have evolved a serine carboxypeptidase-like acyltransferase called littorine synthase (*Ab*LS) which utilizes 1-*O*-β-phenyllactoylglucose formed by a uridine diphosphate (UDP)-dependent glucosyltransferase (UGT) as an acyl donor for tropine to produce littorine (18, 19). The recruitment of two disparate acyltransferase classes for TA biosynthesis in Erythroxylaceae and Solanaceae provides further evidence that these pathways evolved independently between the two plant families. The elucidation of the remaining missing steps in these pathways may reveal insights into the convergent evolution of TA biosynthesis and enable the development of TA drugs and derivatives with novel bioactivity.

TA biosynthesis in Solanaceae has been well characterized owing to well-established tools for pathway manipulation via *Agrobacterium*-mediated transformation (20, 21), RNAi/VIGS knockdown (19), and CRISPR-Cas9 gene knockout techniques (22, 23). Lack of comparable tools for pathway elucidation and tissue culture techniques, the recruitment of novel (or nonhomologous) enzymes compared to those in Solanaceae, and the absence of publicly available *Erythroxylum* genomes complicates the elucidation of the complete Erythroxylaceae TA pathway using traditional approaches.

Brewer's yeast (*Saccharomyces cerevisiae*) is an established host for reconstructing biosynthetic pathways for complex plant alkaloids, including morphinan alkaloids like thebaine and hydrocodone from Papaveraceae (10), monoterpene indole alkaloids like vindoline and catharanthine from Apocynaceae (11), and TAs like hyoscyamine, scopolamine, and their derivatives from Solanaceae (3, 12). In addition to hosting much of the requisite cellular structures (e.g., endoplasmic reticulum) and machinery (e.g., enzyme *N*-glycosylation) to support the heterologous expression of plant-derived enzymes, yeast can be manipulated for high-throughput gene candidate screening and genomic expression of full pathways via well-characterized toolkits (e.g., CRISPR-Cas9) with far shorter design-build-test cycle times relative to conventional plant expression systems (13, 14). Our previous demonstration of solanaceous TA biosynthesis in yeast (3, 12) indicates that it can support the production and analysis of TA intermediates and derivatives.

Here, we develop a yeast platform for the efficient discovery of TA biosynthetic genes from *E. coca* transcriptomes and use this platform to demonstrate that Erythroxylaceae not only recruited different enzymes compared to those in the Solanaceae at several points in the TA pathway, but also evolved novel biosynthetic routes to catalyze the two cyclization steps in the tropane ring formation. We first use metabolomic analysis to show that polyamine levels in *E. coca* leaf extracts are inconsistent with the canonical route to pyrrolidine ring formation via putrescine *N*-methyltransferase (PMT), and characterize the activity of putative *E. coca* polyamine genes in vitro, in planta, and in the yeast discovery platform to demonstrate that the first ring closure in *E. coca* instead occurs through the concerted action of spermidine *N*-methyltransferases (SMTs) and both flavin-and copper-dependent amine oxidases. We then identify a SABATH family methyltransferase with activity on MPOB and a novel CYP81-family monooxygenase that catalyzes the second ring closure to form methylecgonone from *E. coca* transcriptomes, which are collectively responsible for the retention of the carbomethoxy (CMO) group that differentiates Erythroxylaceae TAs from those of Solanaceae. Finally, we show that the newly identified *E. coca* genes complete the biosynthetic pathway for Erythroxylaceae TAs by demonstrating the de novo production of methylecgonine in our engineered yeast platform. Our work provides insights into the diverse biocatalytic strategies that evolved in these plant families for the production of the same class of alkaloids, and may facilitate the development of TA derivatives with novel bioactivities.

Results

The Committed Step of TA Biosynthesis in *E. coca* Proceeds Via Spermidine *N*-methylation. Metabolic profiling of *E. coca* leaf extracts via liquid chromatography and tandem mass spectrometry (LC-MS/MS) revealed the presence of putrescine, spermidine, spermine, and *N*-methylspermidine but not *N*-methylputrescine (NMPUT) in buds, L1 leaves, L2 leaves, and L3 leaves (Fig. 2*A* and *SI Appendix*, Fig. S1)—in contrast to the abundant NMPUT found in TA

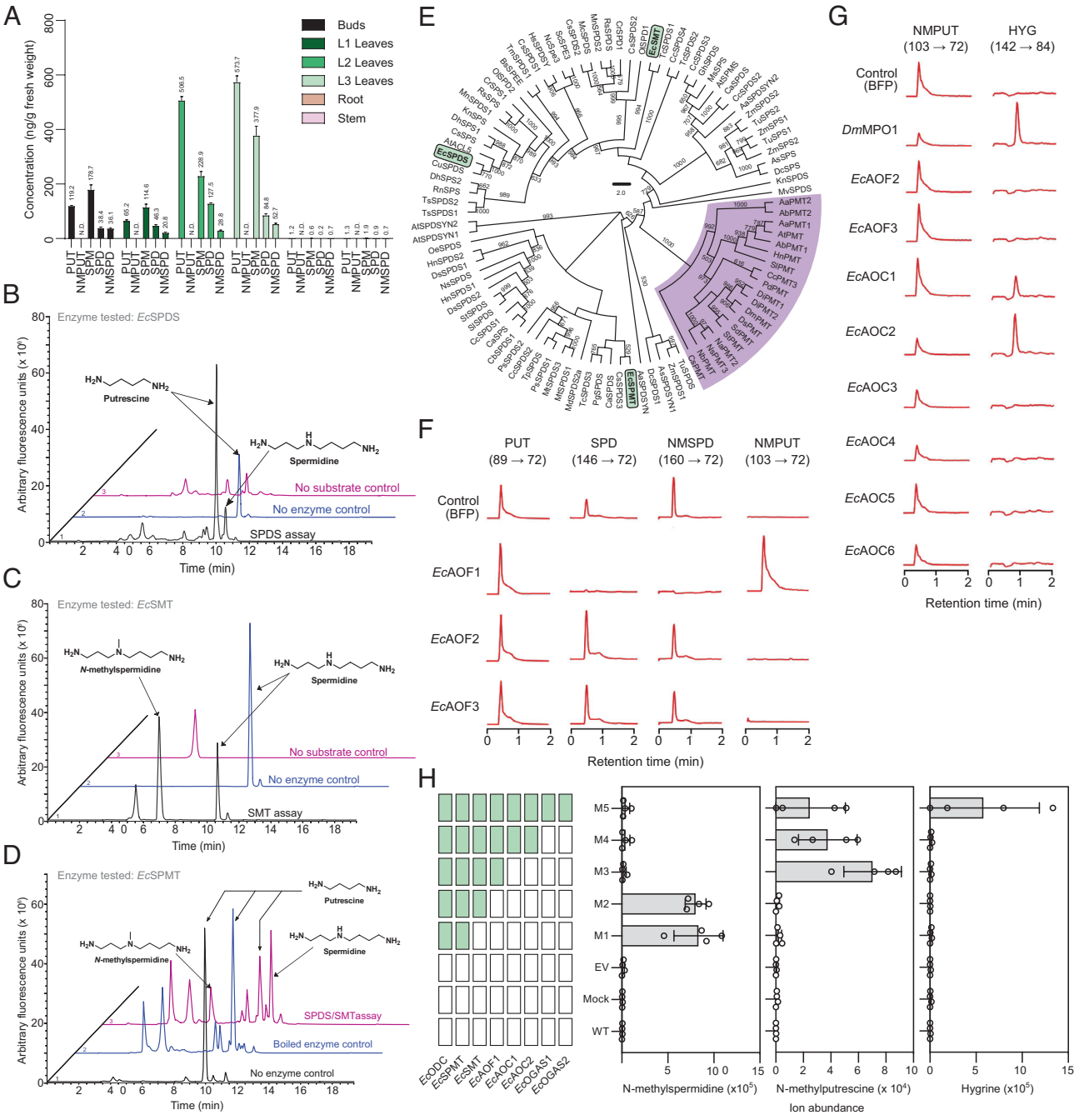

Fig. 2. The pyrrolidine ring in Erythrocylaceae TA biosynthesis is produced via spermidine *N*-methylation. (*A*) Polyamine content in *E. coca* tissues. Polyamines were detected from acidic methanol extracts and are labeled as putrescine (PUT), *N*-methylputrescine (NMPUT), spermine (SPM), spermidine (SPD), and *N*-methylspermidine (NMSPD). Bars and error bars represent the mean and SD of three tissue biological replicates, each with three technical replicates. See *SI Appendix*, Fig. S1 for description of *E. coca* leaf stages. N.D., not detected. (*B*)–(*D*) In vitro enzymatic characterization of purified *E. coca* *Ec*SPDS3/*Ec*SPDS (*B*), *Ec*SPDS1/*Ec*SMT (*C*), and *Ec*SPDS2/*Ec*SPMT (*D*). Before injection, the in vitro enzyme assay samples were derivatized with o-phthalaldehyde (OPA) and fluorenylmethyl chloroformate (FMOC) (see *SI Appendix, Materials and Methods*). Chromatograms are each representative of $n = 5$ independent enzyme assays and peak heights are shown to scale with respect to all other peaks for the same compound. (*B*) High-performance liquid chromatography with fluorescence detection (HPLC-FLD) chromatogram showing SPDS assay with *Ec*SPDS and the aminopropylation cofactor dcSAM. Colors: SPDS assay (black), no enzyme control (blue), no substrate control (pink). (*C*) HPLC-FLD chromatogram of SMT assay with *Ec*SMT and the methylation cofactor SAM. Colors: SMT assay (black), no enzyme control (blue), no substrate control (pink). (*D*) HPLC-FLD chromatogram showing the dual SPDS and SMT activities of *Ec*SPMT in a single overnight enzyme assay containing both aminopropylation and methylation cofactors dcSAM and SAM, respectively. Colors: SPDS/SMT dual assay (pink), boiled enzyme control (blue), no enzyme control (black). (*E*) Dendrogram showing sequence relationships between *Ec*SPDS, *Ec*SMT, and *Ec*SPMT. PMT clade is indicated in magenta, *E. coca* spermidine-associated enzymes identified in this study are highlighted in green. Refer to Dataset S1 for identities and accession numbers of all enzymes in the dendrogram. Values at each junction signify the number of bootstraps out of $n = 1{,}000$ iterations. Scale bar, number of substitutions per amino acid site. Bootstrap values below 500 were not reported. (*F*, *G*) LC-MS/MS multiple reaction monitoring (MRM) chromatogram traces showing the screening of *E. coca* flavin-dependent amine oxidase (AOF) candidates for activity on *N*-methylspermidine (*F*) and *E. coca* copper-dependent amine oxidase (AOC) candidates (*G*) for activity on *N*-methylputrescine in engineered yeast. For (*F*) and (*G*), MS/MS mass transitions used for the identification of PUT, SPD, NMSPD, *N*-methylputrescine (NMPUT), and hygrine (HYG; a proxy for *N*-methylpyrrolinium formation in yeast) are indicated in parentheses. Chromatogram traces are each representative of $n = 3$ biologically independent samples and peak heights are shown to scale with respect to all other peaks for the same compound. (*H*) Validation of the biosynthetic sequence for the first tropane ring formation in *E. coca* via transient co-expression in *N. benthamiana*. Multiple genes were stacked via *A. tumefaciens* vacuum infiltration and analyzed via MRM LC-MS/MS detection of *N*-methylspermidine, *N*-methylputrescine, and hygrine, the spontaneous decarboxylation product of MPOB. WT, wild-type *N. benthamiana* with no agroinfiltration; Mock, control infiltration with infiltration buffer only; EV, empty pHREAC vector control; M1–M5, transient co-expression matrices 1–5 (each matrix is a unique combination of transiently co-expressed genes). Grid on the left side indicates the presence (green) or absence (white) of binary expression vectors for the indicated *E. coca* gene in the *Agrobacterium* co-infiltration matrices. Data indicate the mean of $n = 4$ biologically independent samples (open circles) and error bars show SD.

biosynthetically active tissues of Solanaceae (24). A homology-based search of Erythroxylaceae species for PMT-like sequences failed to yield any close matches, and enzymatic characterization of *E. coca* tissue lysates failed to show PMT activity. Collectively, these metabolite and enzyme activity observations are inconsistent with a biosynthetic route from polyamines to the first ring closure via direct putrescine *N*-methylation as in Solanaceae and—given its abundance in *E. coca* leaves—instead suggest an alternate route in Erythroxylaceae via spermidine. In vitro enzyme assays using crude *E. coca* tissue extracts with spermidine as the substrate revealed *S*-adenosylmethionine (SAM)-dependent conversion to *N*-methylspermidine in L3 and L1 leaves (*SI Appendix*, Figs. S2 and S3), indicating the presence of one or more spermidine *N*-methyltransferases (SMTs). As no SMTs have been reported, we instead used sequences of biochemically characterized solanaceous PMTs, which we hypothesized may be the closest sequence match for SMT, as queries for a tBLASTn search of an in-house transcriptome database of TA biosynthetically active *E. coca* leaf tissues. We identified three full-length protein sequences, which more closely resembled spermidine synthases (SPDS) than PMTs and were thus denoted *Ec*SPDS1-3 (Dataset S1). We cloned *Ec*SPDS1-3 into expression vectors for heterologous expression and purification from *Komagataella phaffii*. Following affinity column purification, proteins were analyzed by SDS-PAGE (*SI Appendix*, Fig. S4–S6), which indicated molecular weights of 39.0, 36.9, and 38.5 kDa for *Ec*SPDS1, 2, and 3, respectively.

Consistent with our observations from crude lysate assays, enzyme assays with purified recombinant *Ec*SPDS1-3 failed to show PMT activity but instead revealed SPDS and SMT activities (Fig. 2 *B*–*D*). Both *Ec*SPDS1 and *Ec*SPDS2 showed SMT activity in which spermidine is methylated at the (internal) N4 position using the co-substrate SAM (Fig. 2 *C* and *D* and *SI Appendix*, Fig. S2), whereas *Ec*SPDS2 and *Ec*SPDS3 exhibited SPDS activity using decarboxylated SAM (dcSAM) as a co-substrate (Fig. 2 *B* and *D*). In particular, *Ec*SPDS2 alone converted putrescine to *N*-methylspermidine when supplied with both dcSAM and SAM (Fig. 2*D*). Based on these observations, we have renamed *Ec*SPDS1, *Ec*SPDS2, and *Ec*SPDS3 to *Ec*SMT, *Ec*SPMT, and *Ec*SPDS, respectively. To elucidate phylogenetic relationships between these enzymes, we performed sequence alignments against biochemically characterized SPDS, spermine synthase (SPS), and PMT sequences and evaluated clustering patterns in the resulting dendrogram (Fig. 2*E*). All characterized PMTs cluster into a separate clade from SPDSs and SPSs, consistent with the proposed early divergence of PMT from the ancestral SPDS family (25, 26). In contrast, there appears to be no clear clustering between characterized SPDSs and SPSs, and all three *E. coca* proteins of interest are dispersed amongst the SPDSs and SPSs, suggesting a more recent evolution in substrate and co-substrate binding motifs.

As TA biosynthesis in *E. coca* is localized to buds, L1 and L2 leaves, we evaluated whether the tissue distribution of the three newly identified *E. coca* polyamine genes is consistent with a role in TA biosynthesis. We measured the relative expression of SAM decarboxylase (*Ec*SAMDC, which supports SPDS activity), *Ec*SMT, *Ec*SPMT, and *Ec*SPDS across *E. coca* tissues by qPCR (*SI Appendix*, Table S1). Expression profiles of *Ec*SAMDC, *Ec*SPMT, and particularly *Ec*SMT are upregulated in buds, L1 and L2 leaves, whereas *Ec*SPDS showed a basal expression level comparable to that of the *Ec*10131 and *Ec*6409 reference genes (27) (*SI Appendix*, Fig. S7). *Ec*SMT and *Ec*SPMT co-expressed strongly across tissues with the established TA genes ornithine decarboxylase (*Ec*ODC) and *Ec*MecgoR (1, 28) (Pearson's correlation coefficient: *Ec*SMT and *Ec*ODC, $r = 0.84$, $P < 0.05$; *Ec*SPMT and *Ec*ODC, $r = 0.81$, $P < 0.10$; *Ec*SMT and *Ec*MecgoR, $r = 0.84$, $P < 0.05$; *Ec*SPMT and *Ec*MecgoR, $r = 0.74$, $P < 0.10$), whereas no correlation was detected for *Ec*SPDS. These observations support a specific role for *Ec*SMT and *Ec*SPMT, but not *Ec*SPDS, in TA biosynthesis and provide further evidence of an alternative biosynthetic route to TAs via spermidine *N*-methylation in *E. coca*.

We developed a testing platform for in vivo characterization of the early *E. coca* TA pathway genes by designing a yeast strain engineered for the overproduction of spermidine. As in *E. coca*, in *S. cerevisiae* spermidine is biosynthesized from the four-carbon diamine putrescine by SPDS (Spe3p), whose aminopropyl donor group is supplied by SAM decarboxylase (Spe2p). To determine whether increased dcSAM availability is needed to support the testing of SPDS in yeast, we overexpressed *SPE2*, *SPE3*, both *SPE2* and *SPE3*, or a blue fluorescent protein (BFP) negative control from low-copy plasmids in a yeast strain (CSY1242) previously engineered for increased accumulation of putrescine via deletion of the polyamine regulatory genes S-methyl-5′-thioadenosine phosphorylase (Meu1p) and ODC antizyme-1 (Oaz1p) coupled with overexpression of glutamate *N*-acetyltransferase (Arg2p), arginase (Car1p), polyamine oxidase (Fms1p), ODC (Spe1p), *Avena sativa* arginine decarboxylase (*As*ADC), and *Escherichia coli* agmatinase (speB) (29). LC-MS/MS analysis of culture supernatants following 72 h growth of transformed strains in selective media revealed a synergistic effect of overexpressing both *SPE2* and *SPE3*, resulting in a 36-fold increase in spermidine levels relative to the BFP control and 3.9- or 12-fold increases relative to overexpression of *SPE2* or *SPE3* alone, respectively (*SI Appendix*, Fig. S8*A*).

We then characterized the activities of the putative SPDSs from *E. coca* (*Ec*SPDS, *Ec*SPMT) in the yeast platform. As *SPE2* potentiates SPDS activity, we co-expressed either *EcSPDS* or *EcSPMT*, native yeast *SPE3*, or a BFP control with *SPE2* from low-copy plasmids in CSY1242. LC-MS/MS analysis of culture supernatants after 72 h growth of transformed strains in selective media indicated that although *Ec*SPMT, like native Spe3p, can function as a SPDS when paired with Spe2p in yeast, *Ec*SPDS does not retain its activity in this context (*SI Appendix*, Fig. S8*B*). We constructed a spermidine overproduction strain (CSY1340) by integrating expression cassettes for *SPE2*, *SPE3*, and *EcSPMT* and disrupting the endogenous SPS gene *SPE4* (which consumes spermidine and whose product spermine is not essential for yeast (15)), in the genome of the previously engineered putrescine overproduction strain CSY1242. We then demonstrated that unlike our previous observations in vitro, *Ec*SMT but not *Ec*SPMT exhibits spermidine *N*-methyltransferase activity when expressed from a low-copy plasmid in CSY1340, as indicated by LC-MS/MS analysis of culture supernatants following 72 h growth of transformed strains in selective media (*SI Appendix*, Fig. S9).

***E. coca* Synthesizes *N*-methyl-Δ^1-pyrrolinium Cation (NMPy) via Spermidine *N*-methylation and Dual Amine Oxidation.** As Erythroxylaceae appear to have evolved one or more *N*-methyltransferases capable of using spermidine instead of putrescine (as in Solanaceae), a novel enzymatic mechanism is required for conversion of *N*-methylspermidine to NMPy, which condenses with 3-oxoglutarate produced by type III polyketide synthases (PYKS or OGAS) to form MPOB in both families (15, 16). If NMPy formation in Erythroxylaceae, like in Solanaceae, proceeds via non-enzymatic cyclization of a methylaminoaldehyde intermediate (e.g., 4-methylaminobutanal), we hypothesized that one or more amine oxidases are required for its biosynthesis from *N*-methylspermidine. Two classes of amine oxidases are found in plants: flavin-dependent amine oxidases (AOFs) catalyze polyamine-shortening (aminopropyl removal) reactions primarily in the cytosol, whereas copper-dependent amine oxidases (AOCs) catalyze the oxidation of primary amine groups to aldehydes in

peroxisomes (30). We identified three AOF (*Ec*AOF1-3) and six AOC (*Ec*AOC1-6) candidates from the transcriptome of *E. coca*. We considered two hypotheses for amine oxidase-catalyzed NMPy formation from *N*-methylspermidine: (i) oxidation of both primary amines to aldehydes to form 4-(methyl(3-oxopropyl)amino)butanal, followed by non-enzymatic intramolecular cyclization to NMPy via retro-Michael addition; or (ii) oxidative shortening of *N*-methylspermidine to *N*-methylputrescine by an AOF, followed by oxidation to 4-methylaminobutanal by an AOC and non-enzymatic cyclization to NMPy (as in Solanaceae).

Both hypotheses for amine oxidase-catalyzed NMPy formation from *N*-methylspermidine were initially tested in the yeast platform. We tested hypothesis (i) by co-expressing each *E. coca* AOF and AOC candidate with *Ec*SMT from low-copy plasmids in the spermidine overproduction yeast strain CSY1340, but observed accumulation of neither 4-(methyl(3-oxopropyl)amino)butanal nor NMPy by LC-MS/MS after 72 h growth of transformed strains. To evaluate hypothesis (ii), we first co-expressed each of *Ec*AOF1-3 or a BFP control with *Ec*SMT in CSY1340 and observed accumulation of *N*-methylputrescine in the strain expressing *Ec*AOF1 (Fig. 2*F*), consistent with a mechanism involving sequential activity of an AOF and AOC. We then screened all six *E. coca* AOC candidates (*Ec*AOC1-6), a copper-dependent *N*-methylputrescine oxidase (MPO) from *Datura metel* previously engineered for improved activity in the yeast peroxisome (denoted *Dm*MPO1) as a positive control, or BFP and the remaining AOF candidates (*Ec*AOF2, *Ec*AOF3) as negative controls via co-expression with *Ec*SMT and *Ec*AOF1 from low-copy plasmids in CSY1340. LC-MS/MS analysis of culture supernatants after 72 h growth in selective media revealed the accumulation of hygrine only in the positive control and in strains expressing either *Ec*AOC1 or *Ec*AOC2 (Fig. 2*G*). Hygrine is a major side product of the first tropane ring formation that can be formed via spontaneous condensation of NMPy with endogenous yeast keto-metabolites (e.g., acetate and acetoacetyl-CoA). We have previously established that because hygrine only accumulates in yeast engineered with the requisite enzymes for NMPy biosynthesis, it can be used as a proxy for NMPy due to its vastly improved MS/MS detectability (31). This result indicated that both *Ec*AOC1 and *Ec*AOC2 are capable of *N*-methylputrescine oxidation to 4-methylaminobutanal and NMPy, supporting hypothesis (ii) that NMPy biosynthesis in *E. coca* proceeds via sequential activity of an AOF (*Ec*AOF1) and an AOC (*Ec*AOC1/2).

Subcellular localization can provide insight into enzymes' functions, and by extension, phylogenetic origins. As plant AOFs and AOCs differ in their canonical subcellular location (30), we verified the localization of the newly identified *E. coca* amine oxidases via fluorescence microscopy of wild-type yeast (CEN.PK2) co-expressing N- or C-terminal GFP fusions of *Ec*AOF1, *Ec*AOC1, or *Ec*AOC2 with a peroxisomal marker (mCherry-Pex3p) from low-copy plasmids. Consistent with its lack of detectable localization signals, *Ec*AOF1-GFP appears to form cytosolic inclusion bodies while GFP-*Ec*AOF1 is soluble and cytosolic (*SI Appendix*, Fig. S10). Consistent with the peroxisomal localization of AOCs like the analogous MPOs in Solanaceae (32), and with the presence of C-terminal peroxisome targeting sequences (PTSs), both GFP-*Ec*AOC1 and GFP-*Ec*AOC2 co-localize with mCherry-Pex3p to yeast peroxisomes, whereas *Ec*AOC1-GFP and *Ec*AOC2-GFP with masked C-terminal PTSs remain in the cytosol (*SI Appendix*, Fig. S10). These results suggest that the newly identified *E. coca* amine oxidases follow the expected pattern of subcellular localization for their associated enzyme families.

To further investigate phylogenetic relationships between the two classes of amine oxidases recruited for TA biosynthesis in Erythroxylaceae, we performed sequence alignments of *Ec*AOF1 and *Ec*AOC1/2 against known AOFs and AOCs, respectively, and evaluated clustering patterns in the resulting dendrograms (*SI Appendix*, Fig. S11). The *N*-methylspermidine oxidase *Ec*AOF1 clusters with other known plant polyamine oxidases, including spermine oxidases isolated from *Arabidopsis thaliana* (48% identity to Q9FNA2) and *Oryza sativa* (50% identity to A0A0P0XM10, 51% identity to Q0J290) and a spermidine oxidase from *Zea mays* (51% identity to O64411) (*SI Appendix*, Fig. S11*A*). The MPOs *Ec*AOC1 and *Ec*AOC2 cluster closely with known copper-dependent amine oxidases (*SI Appendix*, Fig. S11*B*). In particular, *Ec*AOC1 clusters more closely with AOCs from *Malus domestica* (84.35% AA identity to AIS23644.1), *Vitis vinifera* (86.53% AA identity to XP_002273532.2), *Ricinus communis* (85.55% AA identity to XP_002527922.1), *Glycine max* (84.65% AA identity to XP_003551224.1), and *Medicago truncatula* (86.24% AA identity to XP_003613133.2) than with known Solanaceae *N*-methylputrescine or primary amine oxidases from *A. belladonna* (*Ab*MPO2), *Nicotiana sylvestris* (XP_009778427.1), and *Nicotiana tabacum* (BAF49520.1) (*SI Appendix*, Fig. S11*B*). *Ec*AOC2 clusters closely with AOCs from *M. domestica* (83.59% AA identity to AIS23648.1, 84.64% AA identity to AIS23647.1) and *R. communis* (84.63% AA identity to XP_002511334.1). Collectively, these observations are consistent with independent recruitment of both AOF and AOC families for TA biosynthesis in Erythroxylaceae.

To validate the concerted action of previously and newly identified *E. coca* genes implicated in the first tropane ring closure, as well as to verify the observed in vitro dual function of *Ec*SPMT in the context of a plant host, we reconstructed the Erythroxylaceae TA biosynthetic pathway up to NMPy, MPOB, and hygrine via transient co-expression of *E. coca* ODC (*Ec*ODC), *Ec*SPMT, *Ec*SMT, *Ec*AOF1, *Ec*AOC1/2, and/or *Ec*OGAS1/2 in *Nicotiana benthamiana* (Fig. 2*H*). As endogenous putrescine levels in *N. benthamiana* are sufficient to support heterologous TA biosynthesis (33) and ODC overexpression can significantly increase the putrescine pool in transgenic plants (34), we used *Ec*ODC as a co-expression partner gene for all transient transformations. Co-expression of *Ec*ODC and *Ec*SPMT alone was sufficient to enable comparable accumulation of *N*-methylspermidine as when *Ec*SMT was additionally co-expressed. Taken together with our observations in vitro and in yeast, these data confirm that *Ec*SPMT can function as both SPDS and SMT in *E. coca* TA biosynthesis. As in yeast, expression of *Ec*AOF1 enables the conversion of *N*-methylspermidine to *N*-methylputrescine, which is subsequently converted to *N*-methylpyrrolinium and MPOB (as indicated by the product of its spontaneous decarboxylation, hygrine) upon expression of *Ec*AOC1/2 and *Ec*OGAS1/2. Collectively, our results show that the first tropane ring closure in *E. coca* occurs via an alternative biosynthetic route involving bifunctional SPDS/*N*-methyltransferases and a flavin-dependent polyamine oxidase compared to the canonical route via PMT observed in Solanaceae.

A SABATH Methyltransferase Enables 2-CMO Group Retention in Erythroxylaceae TAs. Tian et al. (15) recently reported the characterization of two type III polyketide synthases from *E. novogranatense* (*En*PKS1, *En*PKS2) that catalyze the condensation of two malonyl-CoA units to form 3-oxoglutarate for MPOB biosynthesis. In Solanaceae, CYP82M3-mediated cyclization of MPOB to tropinone coincides with spontaneous decarboxylation of the 2-position. In contrast, retention of the carboxyl group as a 2-carboxymethyl ester in Erythroxylaceae TAs like cocaine implicates a missing methyltransferase—likely of the SABATH family (35)—in the second tropane ring formation step. We searched for SABATH methyltransferases

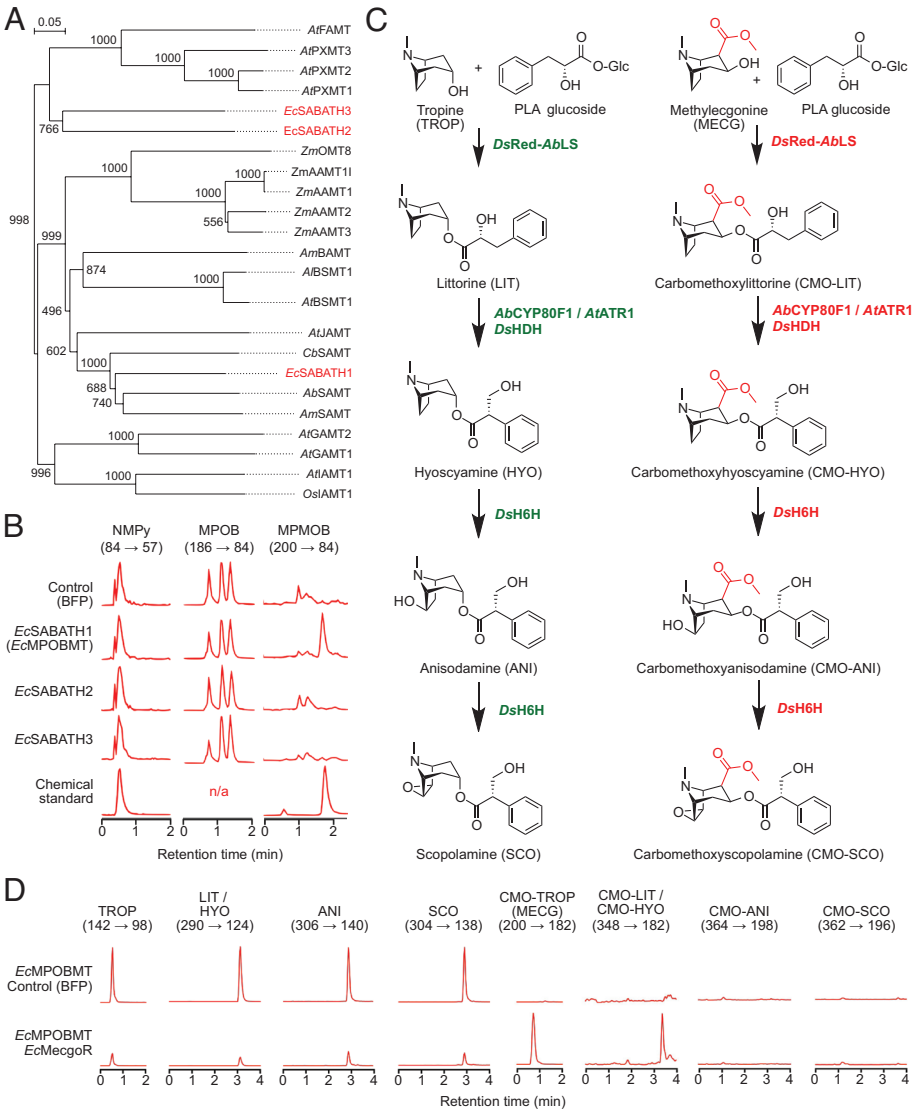

Fig. 3. A SABATH-family methyltransferase enables CMO group retention in Erythroxylaceae TAs. (*A*) Dendrogram showing phylogenetic analysis of three SABATH methyltransferase candidates (red) identified from *E. coca* transcriptome. Previously identified and/or characterized SABATH methyltransferases are indicated in black. Refer to Dataset S1 for identities and accession numbers of all enzymes in the dendrogram. Values at each junction signify the number of bootstraps out of *n* = 1,000 iterations. Scale bar, number of substitutions per amino acid site. (*B*) LC-MS/MS MRM chromatogram traces showing the screening of *E. coca* SABATH methyltransferase candidates for activity on MPOB in engineered yeast. (*C*) Biosynthetic pathway scheme depicting the formation of native Solanaceae TAs (*Left*) and proposed structures of hybrid Solanaceae–Erythroxylaceae CMO-TAs formed via passage of methylecgonine through the Solanaceae TA pathway (*Right*) in engineered yeast. Steps highlighted in green indicated verified activities in engineered yeast, while those in red indicate putative promiscuous activities tested in this experiment. (*D*) LC-MS/MS MRM chromatogram traces showing analysis of the conversion of a Solanaceae TA pathway to one producing hybrid Solanaceae–Erythroxylaceae CMO-TAs in yeast engineered for co-expression of solanaceous TA enzymes with *Ec*MPOBMT and *Ec*MecgoR. Compound name abbreviations correspond to those depicted in panel (*C*). For (*B*) and (*D*), corresponding MS/MS mass transitions used for compound identification are indicated in parentheses. Chromatogram traces are each representative of *n* = 3 biologically independent samples and peak heights are shown to scale with respect to all other peaks for the same compound.

in the transcriptome of *E.* coca using a tBLASTn search with a salicylic acid methyltransferase from *Clarkia breweri* (*Cb*SAMT) and a jasmonic acid methyltransferase from *A. thaliana* (*At*JAMT) as sequence queries, and identified three putative candidates (denoted *Ec*SABATH1-3). Sequence alignments against known SABATH methyltransferases and dendrogram analysis showed that *Ec*SABATH1 clusters closely with previously characterized salicylic acid methyltransferases from multiple species as well as the aforementioned AtJAMT (46.98% AA identity). *Ec*SABATH2 and *Ec*SABATH3 cluster with biochemically characterized paraxanthine methyltransferases from *A. thaliana* (~37% AA identity) (Fig. 3*A*).

To test *Ec*SABATH1-3 for MPOB carboxyl methyltransferase activity, we used a yeast strain (CSY1246) previously engineered to facilitate the screening of gene candidates for the second tropane ring formation step using solanaceous TA enzymes (29). CSY1246 harbors three metabolic modules to support this function (*SI Appendix*, Table S2): Module I increases the accumulation of putrescine via overexpression of glutamate *N*-acetyltransferase (Arg2p), arginase (Car1p), polyamine oxidase (Fms1p), ODC (Spe1p), *A. sativa* arginine decarboxylase (*As*ADC), and *E. coli* agmatinase (speB); Module II-a enables conversion of putrescine to NMPy via *A. belladonna* PMT 1 (*Ab*PMT1) and *D. metel* MPO 1 engineered for improved activity in the yeast peroxisome (*Dm*MPO1); and Module II-b comprises TR I from *D. stramonium* (*Ds*TR1) for conversion of tropinone to tropine, whose detection can be used as an unambiguous positive test if both ring formation steps (e.g., PYKS/OGAS + CYP82M3) are functional.

We first evaluated the heterologous activities of PYKS and OGAS enzymes from Solanaceae (*Ab*PYKS) and Erythroxylaceae (*Ec*OGAS1 and *Ec*OGAS2, *E. coca* homologs of *En*PKS1 and *En*PKS2 (15)) via co-expression with *A. belladonna* tropinone synthase (*Ab*CYP82M3) from low-copy plasmids in CSY1246. LC-MS/MS analysis of culture supernatants following 72 h growth of transformed strains indicated that while all three PYKS/OGAS enzymes are functional in yeast, *Ab*PYKS enables increased flux through MPOB to tropine and is thus a better candidate to support SABATH methyltransferase screening (*SI Appendix*, Fig. S12). We next co-expressed each of the three SABATH methyltransferase candidates or a BFP control with *Ab*PYKS from low-copy plasmids in CSY1246 and analyzed the accumulation of NMPy, MPOB, and MPOB methyl ester (MPMOB) in the culture medium via LC-MS/MS after 72 h growth of transformed strains. Only *Ec*SABATH1 resulted in the production of a molecule whose mass transition ($[M+H]^+$ m/z 200 → 84) and retention time were consistent with that of MPMOB (Fig. 3*B*). Consistent with a role in TA biosynthesis, *Ec*SABATH1 is overexpressed in *E. coca* L1 leaf tissues relative to L2 and L3 leaves (*SI Appendix*, Fig. S13). Thus, we designated *Ec*SABATH1 as the missing MPOB methyltransferase (denoted *Ec*MPOBMT) supporting TA biosynthesis in *E. coca*.

As the tropane moiety of bioactive Solanaceae and Erythroxylaceae TAs differ primarily in the presence of the CMO group, we sought to determine whether expression of *Ec*MPOBMT can convert a biosynthetic pathway for solanaceous TAs into one for Erythroxylaceae-like CMO-TAs. To evaluate the heterologous activity of remaining TA pathway enzyme candidates, we first constructed a MPMOB-producing yeast strain (CSY1341) by integrating expression cassettes for *Ab*PYKS, *Ec*OGAS1, and *Ec*MPOBMT into the genome of the solanaceous NMPy-producing yeast strain CSY1246. We observed that *A. belladonna* tropinone synthase (*Ab*CYP82M3) is tolerant of MPOB methylation and can convert both MPOB to tropinone and MPMOB to methylecgonone when co-expressed with *A. thaliana* NADPH:cytochrome P450 reductase (*At*ATR1) in CSY1341 (*SI Appendix*, Fig. S14). Accordingly, co-expression of these two enzymes with *E. coca* methylecgonone reductase (*Ec*MecgoR) (1) resulted in de novo accumulation of methylecgonine after 72 h growth of transformed strains in selective media (*SI Appendix*, Fig. S14). As *Ds*TR1 and other TRs do not appear to reduce methylecgonone (*SI Appendix*, Fig. S14) (1), we suspected that MPOBMT and MecgoR activities are together sufficient to convert a solanaceous TA pathway into one producing CMO-TAs, although the production of specific CMO-TA esters is dependent on the substrate tolerance of downstream solanaceous TA enzymes (Fig. 3*C*).

We examined the ability of MPOBMT and MecgoR activities combined with solanaceous TA pathway activities to enable CMO-TA production in the yeast platform. We co-expressed *Ec*MPOBMT and *Ec*MecgoR or a BFP control from low-copy plasmids in CSY1297, a yeast strain we previously engineered (31) for de novo biosynthesis of the solanaceous TAs hyoscyamine and scopolamine via three additional metabolic modules: Module III, which enables the production of the solanaceous TA acyl donor phenyllactic acid glucoside from phenylalanine via *Wickerhamia fluorescens* phenylpyruvate reductase (*Wf*PPR) and *A. belladonna* UDP-glucosyltransferase (*Ab*UGT); Module IV, which enables downstream modifications to the TA ester scaffold for conversion of littorine to scopolamine via *A. belladonna* littorine mutase (*Ab*CYP80F1), *D. stramonium* hyoscyamine dehydrogenase (*Ds*HDH), and *D. stramonium* hyoscyamine 6β-hydroxylase/dioxygenase (*Ds*H6H); and Module V, which comprises the acyltransferase littorine synthase from *A. belladonna* engineered for activity in the yeast vacuole via N-terminal fusion of the red fluorescent protein *Ds*Red. Following 96 h growth of the transformed strains in selective media, LC-MS/MS analysis of culture supernatant revealed decreased accumulation of solanaceous TAs and intermediates and substantial accumulation of methylecgonine in CSY1297 expressing both *Ec*MPOBMT and *Ec*MecgoR (Fig. 3*D*). We also observed accumulation of a molecule whose primary mass transition ($[M+H]^+$ m/z 348 → 182) is consistent with that of littorine and/or hyoscyamine ($[M+H]^+$ m/z 290 → 124) with an added CMO group (H [mass = 1] replaced by CMO [mass = 59]) (Fig. 3*D*), suggesting that littorine synthase, littorine mutase and/or hyoscyamine dehydrogenase may have some tolerance for CMO-TA intermediates. Collectively, these data confirm that MPOBMT and MecgoR activities are sufficient to convert a solanaceous TA pathway into one producing Erythroxylaceae-like TAs.

A CYP81-Family Monooxygenase Catalyzes Methylecgonone Ring Closure in *E. coca*. In Solanaceae, cyclization of MPOB to form tropinone requires the cytochrome P450 tropinone synthase (CYP82M3), which is thought to catalyze hydroxylation of the 1 position on MPOB to enable dehydrative iminium formation and intramolecular nucleophilic attack by the β-keto enolate (Fig. 1) (33). We suspected that cyclization of the β-keto acid methyl ester, MPMOB, to methylecgonone in *E. coca* may proceed via a similar mechanism (Fig. 4*A*). Although tropinone synthase also exhibits methylecgonone synthase activity (*SI Appendix*, Fig. S14), no methylecgonone synthase has yet been identified in Erythroxylaceae, and the independent evolution of TA biosynthesis in these families raised the possibility that coca may have recruited an alternate enzyme class for this task.

We performed a homology-based search for *Ab*CYP82M3-like sequences in a 454 transcriptome of *E. coca* and identified five candidate CYP450s (denoted *Ec*CYP1-5) (*SI Appendix*, Fig. S15). As hydroxylation of secondary metabolites in plants may also be performed by 2-oxoglutarate-dependent dioxygenases (2ODDs) (36), we next expanded our search to include more diverse CYP450 families as well as 2ODDs. Using a hierarchical clustering approach, we searched the transcriptomes of three *E. coca* plants (denoted 48, 113, and 124), two *E. novogranatense* plants (denoted 209 and 228), and a low-cocaine-producing *Erythroxylum* species, *Erythroxylum hondense* (37), for CYP450 and 2ODD candidates exhibiting similar patterns of expression across the three species as previously identified Erythroxylaceae TA genes (see *Methods*). This co-expression analysis identified five 2ODD candidates (denoted *Ec*ODD1-5) and 12 additional CYP450 candidates (denoted *Ec*CYP6-17) for testing (Fig. 4*B*). We also included the

Fig. 4. A CYP81-family monooxygenase in *E. coca* enables the conversion of MPMOB to methylecgonone. (*A*) Biosynthetic pathway for screening and characterization of *E. coca* enzyme candidates catalyzing the second ring closure ("cyclases") in engineered yeast. Enzymes in green are expressed from chromosomally integrated gene copies in the cyclase screening yeast strain (CSY1341); enzymes in blue are not used for initial cyclase screening but are expressed from low-copy plasmids for cyclase characterization; enzyme(s) in red represent the missing hydroxylase/cyclase activity expressed from low-copy plasmids in the screening yeast strain. Enzymes in gray are shown for reference as they are part of the cocaine pathway, but are not used in this study. (*B*) Hierarchical clustering heatmap showing expression profiles for cyclase (methylecgonone synthase) gene candidates (vertical axis) identified from Erythroxylaceae transcriptomes across three *E. coca* plants (48, 113, 124), two *E. novogranatense* plants ("*E. novo*" 209, 228), and a low-cocaine-producing *E. hondense* control (horizontal axis). Transcript expression is scaled by row using a normal distribution (z-score). Dendrogram indicates the hierarchical clustering of candidates by expression profile across *E. coca*, *E. novogranatense*, and *E. hondense*. Color scheme for gene IDs: green, known TA pathway genes; red, putative methylecgonone synthase candidates selected for

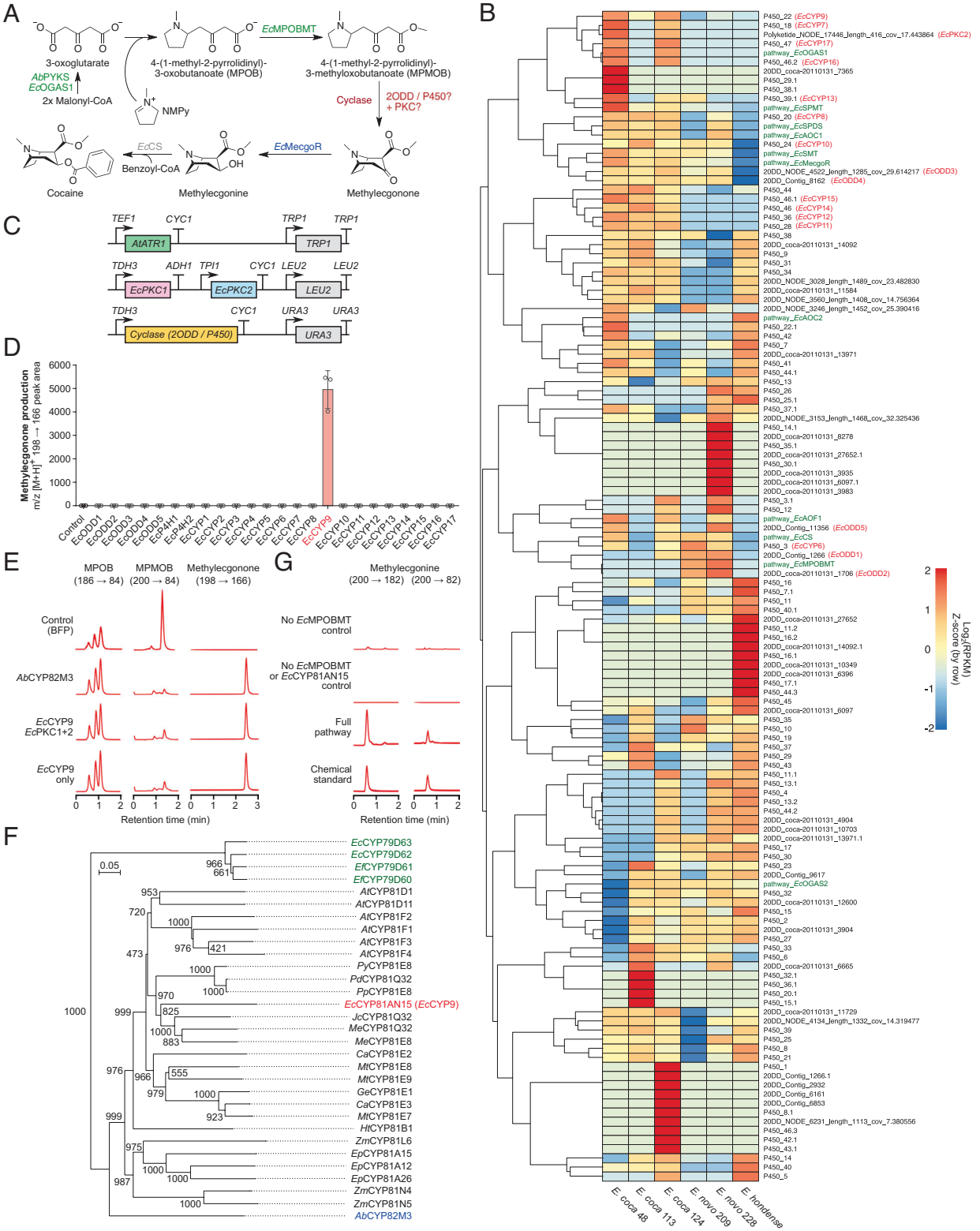

screening. (*C*) Three-plasmid co-expression system used to screen hydroxylase/cyclase candidates for methylecgonone synthase activity in engineered yeast. Each candidate (gold) was co-expressed from a low-copy plasmid with a second plasmid harboring *Arabidopsis* NADPH:CYP450 reductase (*At*ATR1; green) and a third plasmid expressing both *E. coca* PKC-like candidates (pink, blue). (*D*) Methylecgonone production in yeast strains engineered as in (*A*) and (*C*) for co-expression of hydroxylase/cyclase candidates. Strains were cultured in selective media for 72 h at 25°C prior to LC-MS/MS analysis of supernatants. Data indicate the mean of $n = 3$ biologically independent samples (open circles) and error bars show SD. (*E*) LC-MS/MS MRM chromatogram traces of methylecgonone and intermediates detected in the supernatant of negative control and *Ec*CYP9-expressing yeast strains from (*D*). (*F*) Dendrogram showing phylogenetic analysis of methylecgonone synthase (*Ec*CYP81AN15; previously referred to as *Ec*CYP9). Color scheme: red, *Ec*CYP81AN15; black, previously identified CYP81-family enzymes; green, previously characterized *Erythroxylum* aldoxime synthases; blue, *A. belladonna* tropinone synthase. Refer to Dataset S1 for identities and accession numbers of all enzymes in the dendrogram. Values at each junction signify the number of bootstraps out of $n = 1{,}000$ iterations. Scale bar, number of substitutions per amino acid site. (*G*) LC-MS/MS MRM chromatogram traces showing de novo production of methylecgonine via assembly of the core *E. coca* TA biosynthetic pathway in engineered yeast. For (*E*) and (*G*), MS/MS mass transitions used for compound identification are indicated in parentheses. Chromatogram traces are each representative of $n = 3$ biologically independent samples and peak heights are shown to scale with respect to all other peaks for the same compound.

two putative proline 4-hydroxylases found in *E. coca* (*Ec*P4H1-2) whose enzyme family's canonical substrate and activity resemble that of MPMOB hydroxylation (38) for testing. Formation of olivetolic acid via intramolecular cyclization in *Cannabis sativa* requires the concerted activity of a type III polyketide synthase and a small, polyketide cyclase (PKC)-like dimeric α + β barrel (DABB) protein for carboxyl retention (39, 40), suggesting the involvement of a similar PKC in methylecgonone formation in *E. coca*. Thus, we also selected the two PKC-like protein candidates containing DABB-like domains found in the *E. coca* transcriptomes (*Ec*PKC1-2) for investigation.

The candidate hydroxylase and cyclase enzymes were screened in the yeast platform. We co-expressed each of the 24 hydroxylase candidates (*EcODD1-5*, *EcCYP1-17*, *EcP4H1-2*) or a BFP control with the NADPH:cytochrome P450 reductase *AtATR1* and both *Ec*PKC candidates via three low-copy plasmids (Fig. 4*C*) in the MPMOB-producing yeast strain CSY1341 and evaluated accumulation of the expected product, methylecgonone, via LC-MS/MS analysis of culture supernatants after 72 h growth of transformed strains in selective media. One of the 24 candidates, *Ec*CYP9 (denoted methylecgonone synthase), resulted in accumulation of a molecule whose mass transition ($[M+H]^+$ m/z 198 → 166) corresponds to that of methylecgonone (1) (Fig. 4*D*), and whose retention time matches that of the same mass transition peak produced via expression of tropinone synthase (*Ab*CYP82M3) in the same strain (Fig. 4*E*). Unlike with olivetolic acid biosynthesis in *Cannabis*, methylecgonone biosynthesis via *Ec*CYP9 does not appear to require either of the two putative PKCs, as *Ec*CYP9 expression without *Ec*PKC1 and *Ec*PKC2 enabled comparable methylecgonone accumulation (Fig. 4*E*). We analyzed the phylogenetic relationship between the newly identified methylecgonone synthase (*Ec*CYP9), tropinone synthase (CYP82M3), four previously studied *Erythroxylum* oxygenases of the CYP79D family (41), and a panel of sequenced plant CYP450s (Fig. 4*F*). Methylecgonone synthase—which we have designated as *Ec*CYP81AN15 based on its clustering in the CYP81 family—is most closely related to flavonoid/isoflavone 2′-hydroxylases from *Jatropha curcas* (60.4% identity to XP_012079324), *Manihot esculenta* (60% identity to XP_021631824 and 59% identity to XP_021632242), and *Prunus* species (59%, 58%, and 60% identity to XP_007206553, XP_034218022, and PQQ16710, respectively). In contrast, *Ec*CYP81AN15 clusters separately from the four previously characterized *Erythroxylum* CYP79D-family aldoxime synthases (CYP79D60-63) and, consistent with independent recruitment for TA biosynthesis, is only distantly related to *A. belladonna* CYP82M3.

To verify the function of the newly identified *E. coca* genes in their full biosynthetic context, we reconstructed the complete TA pathway for de novo production of methylecgonine in yeast using only Erythroxylaceae genes. We constructed yeast strain CSY1343 by incorporating *E. coca* genes encoding two additional metabolic modules into CSY1340, in which *SPE2*, *SPE3*, and *EcSPMT* are overexpressed and *SPE4* is disrupted to support spermidine overproduction: Module A, enabling conversion of spermidine to MPOB via chromosomally integrated expression cassettes for *EcSMT*, *EcAOF1*, *EcAOC2*, and *EcOGAS1*; and Module B, enabling conversion of MPOB to methylecgonine via low-copy plasmid expression of *EcMPOBMT*, *EcCYP81AN15*, *AtATR1*, and *EcMecgoR*. CSY1343 and two variant strains in which *Ec*MPOBMT and/or *Ec*CYP81AN15 activities are absent were cultured for 96 h in selective media and the culture supernatants were analyzed by LC-MS/MS. We observed de novo production of methylecgonine in the full pathway strain CSY1343 only, validating the function of the core *E. coca* TA pathway in a single host (Fig. 4*G*).

Discussion

This study identifies the remaining TA biosynthetic genes in Erythroxylaceae to reveal that the entire TA pathway is polyphyletic in origin and that its sources in Solanaceae and Erythroxylaceae are independent of one another. Although convergent evolution in plant specialized metabolism is well-documented (42), in most reported cases independent recruitment of non-orthologous genes into analogous pathways occurs with those containing a limited number of enzymatic steps. The more steps necessary for producing a core structure, the greater the requirement for the concomitant selection of duplicated genes for neofunctionalization, and potentially, the greater the time needed for this evolution to occur. One example of the convergent evolution of specialized metabolites in plants is illustrated by the purine alkaloids. Methylation of the purine xanthine to produce caffeine and theobromine is catalyzed by several distantly related SABATH methyltransferases whose recruitment occurred multiple times in different plant lineages, explaining the scattered distribution of these compounds among the angiosperms (43). Another well-documented example of plant alkaloid convergent evolution is found in the biosynthesis of pyrrolizidine alkaloids, for which the enzyme homospermidine synthase was independently recruited at least four times during the evolution of land plants (44). The scattered distribution of TAs across the angiosperms suggests these pathways must have emerged after the development of Eudicots 120 Mya (5). Although the capacity for TA biosynthesis appears to be shared across at least seven plant orders, the phylogenetic relationships between the respective TA pathways outside Solanaceae and Erythroxylaceae are unclear.

Our discovery of *Ec*SMT and *Ec*SPMT provided evidence of the recruitment of SPDS-like enzymes in the formation of *N*-methylputrescine in Erythroxylaceae through an alternative route that differs from the solanaceous TA pathway (Fig. 2 *B* and *D*). In vitro assays of *Ec*SPDS and *Ec*SPMT demonstrated SPDS activity, whereas further evaluation in *S. cerevisiae* revealed that *Ec*SPDS caused depletion of spermidine while *Ec*SPMT maintained SPDS activity. Although the reason for *Ec*SPDS's depletion of spermidine in yeast is unknown, phylogenetic analysis shows that it clusters with Arabidopsis thermospermine synthase (*At*ACL5), suggesting a potential dual role which may explain its spermidine depletion in vivo. *Ec*SPDS and *Ec*SPMT do not cluster together despite sharing SPDS activity, consistent with the possibility that *Ec*SPDS may be involved in primary metabolism while *Ec*SPMT has undergone neofunctionalization for recruitment into the TA pathway. In vitro assays of *Ec*SMT and *Ec*SPMT demonstrated spermidine *N*-methyltransferase activity, whereas in yeast *Ec*SPMT lost SMT activity and only functioned as an SPDS. The exact reason for this discrepancy is unknown but may be related to differences in substrate/cofactor availability and/or in the cellular environment (e.g., post-translational modifications). Subsequent in planta expression of *Ec*SPMT validated its dual SPDS/SMT activity (Fig. 2*H*). Although *Ec*SMT and *Ec*SPMT share SMT activity, *Ec*SMT does not appear to cluster with *Ec*SPMT (49.8% AA identity). *Ec*SPMT's usage of both SAM and dcSAM as cofactors is novel and has not yet been reported for any enzyme in the family. Prior work demonstrated that SPDS1 from *A. thaliana* could gain PMT activity while maintaining SPDS activity by changing two to three amino acids in the active site (26). That mutagenesis can allow an SPDS to bind dcSAM and SAM provides evidence that neofunctionalization and recruitment of novel enzymatic functions are possible with this family of enzymes.

Our observation of SMT activity in *E. coca* is consistent with earlier feeding studies. Radiolabeled feeding studies of *E. coca* leaves

using [5-^{14}C]ornithine demonstrated incorporation through a symmetrical intermediate like putrescine (45). In the context of the newly identified alternate polyamine route, the radiolabeled ornithine is converted to putrescine, incorporated into spermidine, and methylated to form *N*-methylspermidine. The *N*-methylputrescine produced following oxidation in the alternate pathway would therefore exhibit similar equal incorporation patterns. A separate study postulated that spermidine could be a potential intermediate in the production of NMPy (46). Spermidine was labeled asymmetrically in its four-carbon moiety ([6-^{14}C]-1,5,10-triazadecane) and used in feeding studies with *Nicotiana glutinosa*. The degradation analysis revealed the label was incorporated equally at C-2′ and C-5′ of the pyrrolidine rings in nicotine and nornicotine. These results provide evidence that while unusual, spermidine can act as an intermediate in the production of NMPy in both families, and suggest that even within the same family, alternate options for critical early stage intermediates in a pathway can exist.

In contrast to the single amine oxidase involved in Solanaceae TA biosynthesis, our work implicates two amine oxidase families in Erythroxylaceae, providing additional evidence for the convergent evolution of these enzymes. Two classes of amine oxidases exist in plants: those requiring a metal ion cofactor (typically copper) for catalysis and those requiring a covalently bound flavin adenine dinucleotide. Copper-dependent amine oxidases oxidize the carbon adjacent to primary amines resulting in the reduction of molecular oxygen to hydrogen peroxide and producing the corresponding aldehyde and ammonia (47). In Solanaceae, a family-specific subgroup of MPO has evolved from the more general copper-dependent diamine oxidases, important for the formation of lignin and cell wall constituents (31). These MPOs localize to the peroxisome, potentially implicating a transporter to export the *N*-methyl-Δ^1-pyrrolinium cation for further utilization by cytosolic TA enzymes. In contrast, flavin-dependent polyamine oxidases (PAOs) oxidize secondary amines (30). In the case of PAOs localized to the cytosol, the oxidized carbon is located on the exo-side of the N4 atom of spermidine or spermine to produce putrescine or spermidine, respectively, as well as hydrogen peroxide and 3-aminopropanal. *Ec*AOF1 is novel in that it acts on a tertiary amine by oxidizing the carbon on the exo-side of the methylated N4 atom to produce *N*-methylputrescine and 3-aminopropanal. Not only was a novel flavin-dependent oxidase recruited for *E. coca* TA biosynthesis, but a second oxidase was required to convert the newly formed NMPUT to NMPy. *Ec*AOC1 and *Ec*AOC2 were recruited from copper-dependent oxidases within the Erythroxylaceae to catalyze this reaction. EcAOC's closest related family members are all outside the Solanaceae (*SI Appendix*, Fig. S11*B*), providing further evidence for the independent evolution of methylputrescine oxidase activity in angiosperms.

Another line of evidence for the role of repeated evolution in TA biosynthesis was presented in a recent study implicating two type III polyketide synthases (*En*PKS1/2) in the second ring formation step in *E. novogranatense* (15). The equivalent PYKS enzymes in Solanaceae from *Anisodus acutangulus*, *D. stramonium*, *A. belladonna*, and *Solanum lycopersicum* (15, 16) belong to a separate clade from those of the Erythroxylaceae, although both clades perform decarboxylative condensation of two malonyl-CoA subunits to produce 3-oxoglutaric acid. Furthermore, the comparison of the enzyme active site residues reveals significant differences that are consistent with their repeated evolution from ancestral enzymes such as chalcone synthases or stilbene synthases present in their respective lineages. Our data on *Ec*OGAS1/2, the orthologous enzymes to *En*PKS1/2 in *E. coca* (100% AA identity), are also consistent with those reported by Tian et al. (15) and Kim (48).

A unique and definitive feature of Erythroxylaceae TAs is the presence of a 2-CMO group on the tropane ring. Previous chemical analog studies coupled with kinetic binding measurements revealed that the 2-carboymethoxy group is critical for cocaine binding to the dopamine transporter and thus for the subsequent reuptake inhibition of dopamine (49, 50). The absence of MPOB methyltransferase activity in solanaceous plants results in spontaneous decarboxylation of this group during ring closure due to the unstable nature of β-keto acids (51). The resulting TAs have anticholinergic properties but are unable to interact with the dopamine receptor. The recruitment of MPOBMT in coca but not in nightshades may reveal novel insights into the ecological relationships (e.g., plant–herbivore interactions) that shaped the evolution of chemical diversity in these species (52). We postulate that the ancestral methyltransferase for *Ec*MPOBMT was most likely involved in the production of methylsalicylate, an abundant compound in coca leaves (53), as *Ec*MPOBMT clusters with known salicylic acid methyltransferases in the SABATH family (~60% AA identity).

The formation of the second ring in TA biosynthesis most likely proceeds via the formation of an imminium cation similar to NMPy (54). The concomitant oxidation reaction was shown to be catalyzed by a CYP82M3 enzyme (tropinone synthase) in *A. belladonna* (32). We have established that a similar reaction occurs in *E. coca*, although the cytochrome P450 enzyme belongs to the CYP81A family. CYP81A members from *Z. mays* are implicated in the modifications of zealexins (sesquiterpene acids) (55) and other roles for CYP81 members include herbicide resistance in cereals and grasses (56). To date, the only characterized CYP81A members were thought to be lineage-specific, belonging to the monocotyledonous grasses (57). However, our phylogenetic analysis reveals at least several other dicotyledonous families included in this clade. Nonetheless, it is clear that methylecgonone synthase and tropinone synthase have polyphyletic origins.

Consistent with a polyphyletic origin of TA biosynthesis in Erythroxylaceae and Solanaceae, previous work demonstrated that different enzyme classes were also independently recruited to catalyze the terminal esterification steps in these families. Solanaceae evolved a UDP-dependent glucosyltransferase (*Ab*UGT1/UGT84A27) likely recruited from flavonoid metabolism for phenyllactate glucosylation and an acyltransferase recruited from the serine carboxypeptidase-like family (littorine synthase) for condensation of 1-*O*-β-phenyllactoylglucose with tropine to form littorine (19). In contrast, Erythroxylaceae evolved one or more CoA ligases likely recruited from monolignol metabolism (e.g., benzoyl/cinnamoyl/coumaroyl-CoA ligase) for activation of the acyl donor moiety (benzoate/cinnamate) and a BAHD acyltransferase (cocaine synthase) for condensation of the CoA thioester with methylecgonine to form cocaine (18). Further investigation may reveal novel insights into the structural evolution that occurred in these enzymes to enable their recruitment for TA biosynthesis.

Our work highlights the utility of yeast as a discovery platform for high-throughput gene candidate screening, efficient in vivo enzyme characterization, and rapid reconstruction of complex natural product pathways. In addition to advantages in throughput and speed over plant hosts, a yeast platform offers reduced metabolic "cross-talk": because fungi are a more distant biological context for plant enzymes, there is a lower likelihood of native enzymes or metabolites interacting with and confounding measurements of heterologous enzyme activities, enabling greater confidence in the positive identification and classification of new genes relative to in conventional hosts like Arabidopsis or *N. benthamiana*. For example, the initial screening of *E. coca* enzymes involved in the first tropane ring closure in *N. benthamiana* may have been confounded

by its native NMPy/nicotine pathway. Heterologous enzyme testing in yeast may also reveal alternate activity profiles for heterologous enzymes (as was observed for *Ec*SPDS/SPMT/SMT), providing clues for the elucidation of their sequence-structure-function relationships. However, such discrepancies in activity across different hosts also suggest that candidate screening in yeast should be paired with in planta characterization (e.g., *N. benthamiana* or RNAi/VIGS) to validate the function of new enzymes within their native biochemical context. Genomic integration in yeast enables stable gene expression in contrast to transient expression in plants. This provides a potential advantage for reconstructing long plant pathways as blocks of genes that have been discovered, tested, and validated can be integrated, facilitating the screening and testing of the next batch. In contrast, evaluation of a long heterologous pathway in a plant host may require co-infiltration and transient co-expression of more than 10 genes, which can pose practical challenges for consistent pathway expression. With advancements in multiplexed Cas9-mediated genome modification tools, we expect that yeast platforms can complement traditional plant-based approaches for natural product pathway discovery.

Synthetic biology offers a unique opportunity to erase the phylogenetic divisions between biosynthetic pathways across disparate species. By co-expressing key Solanaceae and Erythroxylaceae TA enzymes in a single engineered yeast host, we coupled two analogous pathways that evolved independently over 120 My (1)—and which had never before coexisted in a single organism—resulting in the formation of new-to-nature TAs (Fig. 3*C*, *D*). Future work may reveal that such hybrid natural products share not only structural features of both lineages, but also pharmacological features, enabling access to an unexplored repertoire of medicinal and bioactive compounds using a genetic mix-and-match approach across independently evolved biosynthetic pathways. We expect that leveraging functional genomics, plant-specialized metabolism, and synthetic biology platforms can expand opportunities for the development of new chemical targets across drug discovery, nutrition, and agricultural applications.

Materials and Methods

Detailed materials and methods for all experiments described in this study are provided in *SI Appendix*, *Materials and Methods*.

Plant material. *N. benthamiana* plants (4–6 weeks old) were grown in a greenhouse at 55% humidity, 22°C, and 16-h-light/8-h-dark photoperiod. *E. coca v. coca* plants were grown at 22°C under a 12-h-light/12-h-dark photoperiod, with humidity of 65% and 70%, respectively, and were fertilized weekly with Ferty 3 (15-10-15) and Wuxal Top N (Planta). A voucher specimen was deposited at the Herbarium Haussknecht (JE) at Friedrich Schiller University in Jena, Germany.

De Novo Transcriptome Assembly. Mature leaf transcript profiling on *Erythroxylum* plants grown under greenhouse conditions (identical to those described above) at the United States Department of Agriculture in Beltsville Maryland was constructed by extracting mRNA from *E. hondense*, *E. coca cv coca*, and *E. novogranatense cv novogranatense*. Following library preparation, sequencing was performed using Illumina sequencing and CLC workbench for the assembly of contigs.

Hierarchical Clustering Analysis of *Erythroxylum* Transcriptomes. Hierarchical clustering of methylecgonone synthase candidates from the *Erythroxylum* transcriptome datasets (generated as described in the previous section) was performed using a custom R script (coca_analysis_v1.R), which will be made available on GitHub at the time of publication; the full computational pipeline is described in the *SI Appendix*, *Materials and Methods*.

Phylogenetic Analyses and Dendrograms. Amino acid sequences for all proteins selected for analysis were first aligned using CLUSTAL X2 with default alignment settings and the following clustering parameters: neighbor joining, $n = 1000$ bootstrap trials, random number generator seed = 111. The resulting Phylip format (.phb) tree was transferred to Fig Tree v1.4.4 software for processing.

Statistics. For yeast experiments, biological replicates are defined as independent cultures inoculated from separate yeast colonies or streaks and cultivated in separate containers. For tobacco experiments, one biological replicate is defined as all infiltrated leaves from a single plant. For each transient expression attempt, four biological replicates were used for each gene stacking that was performed.

Data, Materials, and Software Availability. Data supporting the findings of this work are available within the paper and/or SI Appendix. Full sequences of *E. coca* genes newly identified in this work are hosted in GenBank with the following accession numbers: *Ec*SPMT, OP382839; *Ec*SMT, OP382840; *Ec*SPDS, OP382841; *Ec*AOF1, OP382842; *Ec*AOC1, OP382843; *Ec*AOC2, OP382844; *Ec*OGAS1, OP382845; *Ec*OGAS2, OP382846; *Ec*MPOBMT, OP382847; *Ec*CYP81AN15, OP382848. The custom R scripts used for hierarchical clustering analysis of Erythroxylaceae transcriptome datasets will be available at the time of publication on the Smolke Laboratory GitHub repository (https://github.com/smolkelab/coca_coexpression_analysis).

ACKNOWLEDGMENTS. We thank the greenhouse staff of the Max Planck Institute for Chemical Ecology and the staff at the Leibniz Institute for Plant Genetics and Crop Plant Research for the rearing and care of the plants involved in this study. We thank Dr. Mohammed-Reza Hajirezaei (IPK) for assistance with LC-MS measurements; Dr. A. Cravens (Stanford University) for the yeast multiplex CRISPR–Cas9/sgRNA plasmids used for yeast genomic modifications; and the Stanford Cell Sciences Imaging Facility for access to microscopy equipment and training. We thank Dr. Birgit Dräger for the generous donation of synthesized dcSAM for in vitro enzyme assays. We thank Kyle Glockzin for his help with data collection and discussion. This work was supported by an Alexander von Humboldt postdoctoral fellowship to J.C.D., the NSF (NSF-1714236 grant to J.C.D.), the NIH (AT007886 grant to C.D.S.), the Chan Zuckerberg Biohub (C.D.S. is a Chan Zuckerberg Biohub investigator), the Siebel Scholars Foundation (doctoral fellowship to P.S.) and the Natural Sciences and Engineering Research Council of Canada (doctoral postgraduate scholarship to P.S.).

Author affiliations: [a]Department of Molecular Genetics, Leibniz Institute for Plant Genetics and Crop Plant Research (IPK) Ortsteil Gatersleben, Seeland D-06466, Germany; [b]Department of Bioengineering, Stanford University, Stanford, CA 94305; [c]Department of Chemistry and Biochemistry, Texas Tech University, Lubbock, TX 79409; [d]Department of Biochemistry, Max Planck Institute for Chemical Ecology, Jena, D-07745, Germany; [e]U.S. Department of Agriculture-Agricultural Research Service, Sustainable Perennial Crops Laboratory, Beltsville, MD 20705; and [f]Chan Zuckerberg Biohub, San Francisco, CA 94158

1. J. Jirschitzka *et al.*, Plant tropane alkaloid biosynthesis evolved independently in the Solanaceae and Erythroxylaceae. *Proc. Natl. Acad. Sci. U.S.A.* **109**, 10304–10309 (2012).
2. M. Lounasmaa, T. Tamminen, "The tropane alkaloids" in *The Alkaloids: Chemistry and Pharmacology*, G. A. Cordell, Ed. (Academic Press, 1993), pp. 1–114.
3. P-A. Nocquet, T. Opatz, Total synthesis of (±)-scopolamine: challenges of the tropane ring. *Eur. J. Org. Chem.* **2016**, 1156–1164 (2016).
4. P. C. Meltzer, Y. Anna, Bertha Liang, K. Madras, The discovery of an unusually selective and novel cocaine analog: Difluoropine. Synthesis and inhibition of binding at cocaine recognition sites. *J. Med. Chem.* **37**, 2001–2010 (1994).
5. N. Kim, O. Estrada, B. Chavez, C. Stewart, J. C. D'Auria, Tropane and granatane alkaloid biosynthesis: A systematic analysis. *Molecules* **21**, (2016).
6. T. Schmeller, F. Sporer, M. Sauerwein, M. Wink, Binding of tropane alkaloids to nicotinic and muscarinic acetylcholine receptors. *Pharmazie* **50**, 493–495 (1995).
7. T. Plowman, The Ethnobotany of Coca (*Erythroxylum spp., Erythroxylaceae*). *Adv. Econ. Bot.* **1**, 62–111 (1984).
8. T. Plowman, L. Rivier, Cocaine and cinnamoylcocaine content of *erythroxylum* Species. *Ann. Bot.* **51**, 641–659 (1983).
9. T. Plowman, Amazonian coca. *J. Ethnopharmacol.* **3**, 195–225 (1981).
10. F. I. Carroll *et al.*, Probes for the cocaine receptor. Potentially irreversible ligands for the dopamine transporter. *J. Med. Chem.* **35**, 1813–1817 (1992).
11. S. Kelkar *et al.*, Synthesis, Cocaine receptor affinity, and dopamine uptake inhibition of several new 2.beta.-substituted 3.beta.-phenyltropanes. *J. Med. Chem.*, (September 6, 2022).

12. F. I. Carroll, A. H. Lewin, J. W. Boja, M. J. Kuhar, Cocaine receptor: Biochemical characterization and structure-activity relationships of cocaine analogs at the dopamine transporter. *J. Med. Chem.* **35**, 969–981 (1992).
13. F. Bai *et al.*, Overexpression of the AbSAUR1 gene enhanced biomass production and alkaloid yield in *Atropa belladonna*. *Ind. Crops Prod.* **140**, 111705. (2019).
14. World Health Organization, "*World Health Organization Model List of Essential Medicines: 21st List 2019*" (World Health Organization, 2019).
15. T. Tian *et al.*, Catalytic innovation underlies independent recruitment of polyketide synthases in cocaine and hyoscyamine biosynthesis. *Nat. Commun.* **13**, 4994 (2022).
16. J.-P. Huang *et al.*, Tropane alkaloids biosynthesis involves an unusual type III polyketide synthase and non-enzymatic condensation. *Nat. Commun.* **10**, 4036 (2019).
17. J. C. D'Auria, Acyltransferases in plants: A good time to be BAHD. *Curr. Opin. Plant Biol.* **9**, 331–340 (2006).
18. G. W. Schmidt *et al.*, The last step in cocaine biosynthesis is catalyzed by a BAHD acyltransferase. *Plant Physiol.* **167**, 89–101 (2015).
19. F. Qiu *et al.*, Functional genomics analysis reveals two novel genes required for littorine biosynthesis. *New Phytol.* **225**, 1906–1914 (2020).
20. G. Song, A. Walworth, *Agrobacterium tumefaciens*-mediated transformation of *Atropa belladonna*. *Plant Cell Tissue Organ Cult. PCTOC* **115**, 107–113 (2013).
21. A. C. Rajewski, K. B. Elkins, A. Henry, J. Van Eck, A. Litt, In vitro plant regeneration and *Agrobacterium tumefaciens*–mediated transformation of *Datura stramonium* (Solanaceae). *Appl. Plant Sci.* **7**, e01220. (2019).
22. L. Zeng *et al.*, Development of *Atropa belladonna* L. plants with high-yield hyoscyamine and without its derivatives using the CRISPR/Cas9 system. *Int. J. Mol. Sci.* **22**, 1731 (2021).
23. F. Hasebe *et al.*, CRISPR/Cas9-mediated disruption of the PYRROLIDINE KETIDE SYNTHASE gene reduces the accumulation of tropane alkaloids in *Atropa belladonna* hairy roots. *Biosci. Biotechnol. Biochem.* **85**, 2404–2409 (2021).
24. T. Zhao *et al.*, Ornithine decarboxylase regulates putrescine-related metabolism and pollen development in Atropa belladonna. *Plant Physiol. Biochem. PPB* **192**, 110–119 (2022).
25. S. Biastoff, N. Reinhardt, V. Reva, W. Brandt, B. Drager, Evolution of putrescine *N*-methyltransferase from spermidine synthase demanded alterations in substrate binding. *FEBS Lett.* **583**, 3367–74 (2009).
26. A. Junker, J. Fischer, Y. Sichhart, W. Brandt, B. Dräger, Evolution of the key alkaloid enzyme putrescine *N*-methyltransferase from spermidine synthase. *Front. Plant Sci.* **4**, 260 (2013).
27. T. Docimo, G. W. Schmidt, K. Luck, S. K. Delaney, J. C. D'Auria, Selection and validation of reference genes for quantitative gene expression studies in *Erythroxylum coca* (2013), https://doi.org/10.12688/f1000research.2-37.v1 (September 7, 2022).
28. T. Docimo *et al.*, The first step in the biosynthesis of cocaine in *Erythroxylum coca*: The characterization of arginine and ornithine decarboxylases. *Plant Mol. Biol.* **78**, 599–615 (2012).
29. P. Srinivasan, C. D. Smolke, Engineering a microbial biosynthesis platform for de novo production of tropane alkaloids. *Nat. Commun.* **10**, 1–15 (2019).
30. P. Tavladoraki, A. Cona, R. Angelini, Copper-containing amine oxidases and FAD-dependent polyamine oxidases are key players in plant tissue differentiation and organ development. *Front. Plant Sci.* **7**, (2016).
31. M. Naconsie, K. Kato, T. Shoji, T. Hashimoto, Molecular evolution of *N*-methylputrescine oxidase in tobacco. *Plant Cell Physiol.* **55**, 436–444 (2014).
32. M. A. Bedewitz, A. D. Jones, J. C. D'Auria, C. S. Barry, Tropinone synthesis via an atypical polyketide synthase and P450-mediated cyclization. *Nat. Commun.* **9**, 5281 (2018).
33. T. Zhao *et al.*, Engineering tropane alkaloid production based on metabolic characterization of ornithine decarboxylase in Atropa belladonna. *ACS Synth. Biol.* **9**, (2020).
34. J. C. D'Auria, F. Chen, E. Pichersky, "The SABATH family of MTs in *Arabidopsis thaliana* and other plant species" in *Recent Advances in Phytochemistry, Integrative Phytochemistry: From Ethnobotany to Molecular Ecology*, J. T. Romeo, Ed. (Elsevier, 2003), pp. 253–283.
35. P. Srinivasan, C. D. Smolke, Biosynthesis of medicinal tropane alkaloids in yeast. *Nature* **585**, 614–619 (2020).
36. Y. Kawai, E. Ono, M. Mizutani, Evolution and diversity of the 2-oxoglutarate-dependent dioxygenase superfamily in plants. *Plant J. Cell Mol. Biol.* **78**, 328–343 (2014).
37. S. Bieri, A. Brachet, J.-L. Veuthey, P. Christen, Cocaine distribution in wild Erythroxylum species. *J. Ethnopharmacol.* **103**, 439–447 (2006).
38. K. L. Gorres, R. T. Raines, Prolyl 4-hydroxylase. *Crit. Rev. Biochem. Mol. Biol.* **45**, 106–124 (2010).
39. S. J. Gagne *et al.*, Identification of olivetolic acid cyclase from *Cannabis sativa* reveals a unique catalytic route to plant polyketides. *Proc. Natl. Acad. Sci. U. S. A.* **109**, 12811–12816 (2012).
40. X. Yang *et al.*, Structural basis for olivetolic acid formation by a polyketide cyclase from *Cannabis sativa*. *FEBS J.* **283**, 1088–1106 (2016).
41. K. Luck *et al.*, CYP79D enzymes contribute to jasmonic acid-induced formation of aldoximes and other nitrogenous volatiles in two *Erythroxylum* species. *BMC Plant Biol.* **16**, 215 (2016).
42. E. Pichersky, E. Lewinsohn, Convergent evolution in plant specialized metabolism. *Annu. Rev. Plant Biol.* **62**, 549–566 (2011).
43. R. Huang, A. J. O'Donnell, J. J. Barboline, T. J. Barkman, Convergent evolution of caffeine in plants by co-option of exapted ancestral enzymes. *Proc. Natl. Acad. Sci. U.S.A.* **113**, 10613–10618 (2016).
44. D. Ober, E. Kaltenegger, Pyrrolizidine alkaloid biosynthesis, evolution of a pathway in plant secondary metabolism. *Phytochemistry* **70**, 1687–1695 (2009).
45. E. Leete, Biosynthesis of the pyrrolidine rings of cocaine and cuscohygrine from [5-14C]-ornithine via a symmetrical intermediate. *J. Am. Chem. Soc.* **104**, 1403–1408 (1982).
46. E. Leete, Spermidine: An indirect precursor of the pyrrolidine rings of nicotine and nornicotine in *Nicotiana glutinosa*. *Phytochemistry* **24**, 957–960 (1985).
47. I. Fraudentali *et al.*, The copper amine oxidase AtCuAOδ participates in abscisic acid-induced stomatal closure in Arabidopsis. *Plants* **8**, 183 (2019).
48. N. Kim, "*Tropane Alkaloid Biosynthesis in Erythroxylum coca Involves an Atypical Type III Polyketide Synthase*" (Texas Tech University, Lubbock, TX, 2020).
49. K. C. Schmitt *et al.*, Interaction of cocaine-, benztropine-, and GBR12909-like compounds with wild-type and mutant human dopamine transporters: Molecular features that differentially determine antagonist-binding properties. *J. Neurochem.* **107**, 928–940 (2008).
50. J. D. Elsworth, J. R. Taylor, P. Jatlow, R. H. Roth, Serotonin involvement in cocaine sensitization: Clues from studies with cocaine analogs. *Drug Dev. Res.* **30**, 189–200 (1993).
51. J. Lohman, L. Stunkard, A. Benjamin, T. Boram, Exploring enzymatic β-keto acid (de)carboxylation with malonyl-CoA analogs. *FASEB J.* **33**, 633.17–633.17 (2019).
52. J. Jirschitzka, "*The Final Steps of Cocaine Biosynthesis in the Erythroxylaceae Provide Insight into the Biochemistry, Physiology and Evolution of Tropane Alkaloid Biosynthesis*" (Friedrich-Schiller-Universität Jena, Jena, Germany, 2014).
53. M. Novák, C. Salemink, The Essential Oil of Erythroxylum coca. *Planta Med.* **53**, 113–113 (1987).
54. N. Kim, B. Chavez, C. Stewart, J. C. D'Auria, "Structure and function of enzymes involved in the biosynthesis of tropane alkaloids" in *Tropane Alkaloids: Pathways, Potential and Biotechnological Applications*, V. Srivastava, S. Mehrotra, S. Mishra, Eds. (Springer, 2021), pp. 21–50.
55. Y. Ding *et al.*, Genetic elucidation of interconnected antibiotic pathways mediating maize innate immunity. *Nat. Plants* **6**, 1375–1388 (2020).
56. C. C. Hansen, D. R. Nelson, B. L. Møller, D. Werck-Reichhart, Plant cytochrome P450 plasticity and evolution. *Mol. Plant* **14**, 1244–1265 (2021).
57. S. Iwakami *et al.*, Cytochrome P450 CYP81A12 and CYP81A21 are associated with resistance to two acetolactate synthase inhibitors in *echinochloa phyllopogon*. *Plant Physiol.* **165**, 618–629 (2014).